photonics

MDPI

Article

Analysis of the Effective and Actual Lens Position by Different Formulas. Postoperative Application of a Ray-Tracing-Based Simulated Optical Model

Diana Gargallo Yebra [1,*], Laura Remón Martín [1], Iván Pérez Escorza [1] and Francisco Javier Castro Alonso [2,3]

[1] Department of Applied Physics, University of Zaragoza, 50009 Zaragoza, Spain; lauremar@unizar.es (L.R.M.)
[2] Department of Ophthalmology, Alcañiz Hospital, 44600 Alcañiz, Spain
[3] GIMSO, Institute for Health Research Aragón, Hospital Universitario Miguel Servet, 50009 Zaragoza, Spain
* Correspondence: dgargallo@unizar.es

Abstract: (1) Background: This study compares the effective lens position (ELP) and intraocular lens power (IOLP) derived from SRK/T, Hoffer Q, Holladay I, and Haigis formulas with the actual lens position (ALP) and the implanted IOLP after cataract surgery. Additionally, it aims to optimize ALP using a ray-tracing-based simulated optical model to achieve emmetropia. (2) Methods: A retrospective observational study was conducted on 43 eyes implanted with the same monofocal intraocular lens (IOL). Preoperative and postoperative biometric data were collected using the Lenstar LS900. Postoperative measurements included ALP, subjective refraction, and refraction error (RE). Optical simulations (OSLO EDU 6.6.0) were utilized to optimize ALP for emmetropia (ALP_{IDEAL}). (3) Results: Paired *t*-test results between RE_{OSLO}-RE_{OBJ} (*p*-value = 0.660) and RE_{OSLO}-RE_{SUB} (*p*-value = 0.789) indicated no significant statistical differences. However, statistically significant differences were found between ALP and ALP_{IDEAL} ($p < 0.05$), with a difference of -0.04 ± 0.45 mm [ranging from -1.00 to 1.20 mm]. A significant correlation was observed between ΔALP ($\Delta ALP = ALP - ALP_{IDEAL}$) and RE_{SUBJ}. (4) Conclusions: This customized ray-tracing eye model effectively achieves refractive outcomes similar to those obtained both subjectively and objectively post-surgery. Additionally, it has enabled optical simulations to optimize the IOL position and achieve emmetropia.

Keywords: effective lens position; actual lens position; cataract; ray-tracing; intraocular lens; refractive error

Citation: Gargallo Yebra, D.; Remón Martín, L.; Pérez Escorza, I.; Castro Alonso, F.J. Analysis of the Effective and Actual Lens Position by Different Formulas. Postoperative Application of a Ray-Tracing-Based Simulated Optical Model. *Photonics* **2024**, *11*, 711. https://doi.org/10.3390/photonics11080711

Received: 11 June 2024
Revised: 23 July 2024
Accepted: 25 July 2024
Published: 30 July 2024

1. Introduction

Cataract surgery is now considered a type of refractive surgery, and patients have high expectations for achieving optimal visual outcomes to enhance their quality of life [1]. The individual selection of the optimal intraocular lens power (IOLP) is crucial to visual quality optimization after cataract surgery. In current practice, the IOLP is calculated by using statistical regression or theoretical formulas. Theoretical formulas have used different approaches to estimate the effective lens position (ELP). ELP, defined as the distance from the anterior surface of the cornea to the lens plane, assuming the lens is infinitely thin, is used to calculate IOLP. It is considered that 40% of the postoperative refractive error (RE) is due to an inaccurate prediction of ELP and is considered the leading source of postoperative errors [2,3].

The first generation of theoretical formulas assumed a constant ELP; the second generation replaced the constant ELP with a variable dependent on the axial length (AL). Third-generation formulas, such as SRK/T [4], Holladay I [5] or Hoffer Q [6], used AL and keratometry (K) to increase the accuracy of ELP prediction. New generation formulas, such as Barrett Universal II [7], Haigis [8], Holladay II, Olsen [9], and EVO, take more variables into account, such as lens thickness (LT), anterior chamber depth (ACD), white-to-white (WTW), age, and preoperative refraction. New generation formulas are not

public, and thus their estimated ELP remains unknown. Formulas based on ray tracing calculations [10], artificial intelligence [11], or combinations of different methodologies [12] have been proposed recently, for instance, Hill-RBF, Kane, Pearl-DGS, or Karmona. Several studies [13,14] have reported good refractive outcomes with these new generation formulas, but there is no consensus on which is the most accurate method, especially in the most complex cases.

Deviation in ELP from the postoperative actual lens position (ALP, distance from the corneal epithelium to the anterior surface of the IOL) represents the largest source of error in modern IOLP calculation formulas [3]. Currently, optical coherence tomography and some optical biometers can be used to measure ALP. Lenstar LS 900 (Haag-Streit AG, Koeniz, Switzerland) is an optical biometry device that utilizes optical low coherence reflectometry [15] to measure different ocular biometric parameters in a single shot with excellent repeatability and reproducibility [16]. Knowledge on how ALP differs from ELP could be used to optimize ELP predictions, leading to better IOLP estimations and improved refractive and visual outcomes.

In the present study, we evaluated the utility of OSLO, an advanced optical tool, for designing numerical models of a pseudophakic eye based on the real ocular parameters (biometry and keratometric data) measured to accurately calculate the ideal IOL positions. By using OSLO, we aim to optimize the estimation of IOL position and improve refractive outcomes after cataract surgery.

2. Methods

2.1. Subjects and Procedures

This retrospective, observational study consisted of 43 eyes of 43 patients who had already undergone uneventful phacoemulsification with IOL implantation at Hospital Alcañiz between September 2021 and November 2022. The study was conducted in accordance with the Declaration of Helsinki and approved by the Aragon Research Ethics Committee (CEICA). The nature of the study was explained to all patients, and they signed an informed consent. All patients provided written, informed consent for publication.

Inclusion criteria were availability of preoperative ocular biometry measurements from Lenstar, suitability for Alcon Clareon monofocal IOL (Alcon Laboratories, Dallas, TX, USA) implantation in the capsular bag, and absence of complications during or after cataract surgery. Exclusion criteria were preoperative corneal astigmatism greater than 2.00 diopters (D), eyes with AL below 22 mm or over 26 mm, previous ocular surgery, ocular trauma, active ocular infection or inflammation, and the impossibility of IOL detection with Lenstar. If both eyes of a patient met the inclusion criteria, one eye was randomly selected for the study. The sample size was derived based on calculations and evaluation of the optimization of ALP to achieve emmetropia [17]. The same methodology applied to the current work suggested that a sample size of at least 16 participants would yield 90% power to optimize the position of the IOL and the refractive error at the 0.05 significance level.

Preoperatively and postoperatively (at 4–5 weeks after the surgery), central corneal thickness (CCT), K, ACD, LT, AL, and WTW were retrieved from the measurements obtained with the Lenstar system. The tomography obtained with the Pentacam HR (Oculus, Wetzlar, Germany) was used for collecting data, including anterior and posterior corneal radii and asphericities of both surfaces. Additionally, postoperatively, Lenstar optical biometry in "pseudophakic" mode was performed to determine the ALP. An objective refractive error (RE_{OBJ}) was performed using the Topcon autorefractometer, and the subjective refractive error (RE_{SUBJ}) was performed by the same experienced examiner (I.P.E) under the same conditions to avoid any influence on the results.

2.2. Surgery Procedure

The same surgeon (F.J.C.A.) performed all surgeries under topical anesthesia. A 5.5 mm continuous curvilinear capsulorhexis and a 2.4 mm clear temporal corneal microincision were made for the cataract procedure. The Clareon monofocal IOL, an acrylic hydrophobic

material, was implanted in the capsular bag using the AutonoMe single-use injection system (Alcon). Its optic design induced a −0.20 µm spherical aberration of 6.00 mm on the anterior surface. Preoperative IOLP calculation was carried out with the Barrett Universal II formula, aiming for emmetropia with a manufacturer-labeled A-Constant of 119.1.

2.3. IOLP and ELP Calculation

Using the preoperative biometric data parameters, the IOLP and ELP were predicted using four formulas: Hoffer Q, Holladay I, SRK/T, and Haigis. These theoretical formulas are based on the multiple regression of the A-Constant, K and AL in Hoffer Q, Holladay I, SRK/T and ACD in Haigis. The constant lenses used were 5.64 for Hoffer Q, 1.84 for Holladay I, 119.1 for the SRK/T, a0 = −0.769, a1 = 0.234, a2 = 0.217 for Haigis.

2.4. Optical Modeling

In addition to the clinical study, optical simulations were conducted to estimate the postoperative refractive error (RE_{OSLO}) in terms of the spherical equivalent of the IOL after surgery. For the optical simulations, 43 numerical models of a pseudophakic eye based on the real ocular parameters (biometry and keratometric data) were created using commercial optical design software (OSLO EDU v.6.6.0, Lambda Research Corporation, Groton Rd, Westford, United States). The procedure to generate the pseudophakic eyes consisted of three main steps (Figure 1):

(1) Firstly, Clareon IOL was designed with a power range between 16.50 and 26.50 D and a spherical aberration on the anterior surface equal to −0.20 µm for a 6.00 mm pupil.
(2) Secondly, all real eyes were modeled using the refractive index values of the Atchison model eye [18]. To model each cornea, we used the postoperative tomography measurements obtained with Pentacam. The postoperative values of CCT, ALP, and AL were obtained from the Lenstar, and the position of the iris in each case was assumed from the measurement of the preoperative ACD with the Lenstar, which represented the distance from the anterior corneal vertex to the position of the crystalline lens.
(3) Thirdly, the operated eyes were simulated in the software, including the IOLP and the ALP.

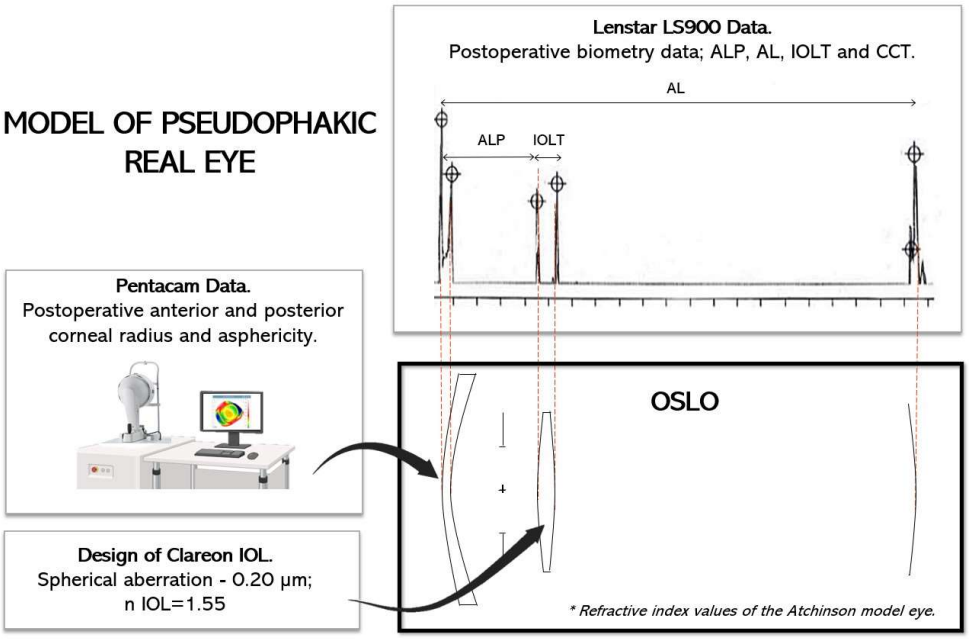

Figure 1. Model of pseudophakic real eye using OSLO.

RE_{OSLO} was determined using Zernike coefficients [19,20] from wavefront aberration analysis at 587 nm wavelength and 3 mm pupil diameter. The "refractive Zernike power polynomials" from Iskander et al.'s study [21] were employed to derive the sphero-cylindrical refraction. The following equations were applied to obtain the diopter vector components of residual refractive error that achieve minimum RMS wavefront error at the entrance's pupil plane:

$$M = \frac{-4\sqrt{3}\, C_2^0}{R^2}$$

$$J_0 = \frac{-2\sqrt{6}\, C_2^2}{R^2}$$

$$J_{45} = \frac{-2\sqrt{6}\, C_2^{-2}}{R^2}$$

where M denotes the average spherical error, J_0 and J_{45} indicate the components of astigmatism and oblique astigmatism, respectively, C_2^0 is the Zernike defocus coefficient, C_2^2 is the Zernike astigmatism, and C_2^{-2} is the Zernike oblique astigmatism coefficient (all in μm), and R is the aperture radius (in mm) of the entrance pupil's system. The residual sphero-cylindrical refraction in minus-cylinder form was obtained with the following equations:

$$cyl = -2\sqrt{{J_0}^2 + {J_{45}}^2}$$

$$sph = M - \frac{cyl}{2}$$

where *sph* and *cyl* are the spherical and cylindrical components, respectively, of the residual sphero-cylindrical correction at the entrance pupil plane.

After the eyes were modeled, the ideal position of the IOL (ALP_{IDEAL}) to achieve emmetropia, i.e., when the Root Mean Square would be zero, was determined. The difference between ALP and ALP_{IDEAL} was called ΔALP ($\Delta ALP = ALP - ALP_{IDEAL}$).

2.5. Data Analysis

A statistical analysis was conducted using R-Commander version 4.1.1 statistical software. The data's normality was tested with the Shapiro–Wilk test, which did not reject normality ($p > 0.05$). Subsequently, a paired *t*-test was used to compare the means of related samples, identifying significant differences between them. Calculations were made for differences (mean dif.) between IOLP and ELP with each formula: postoperative objective refractive error (RE_{OBJ}), subjective refractive error (RE_{SUBJ}), and OSLO-derived refractive error (RE_{OSLO}). Bland–Altman plots were used to explore the correlation between ELP, ALP, and RE measurements. Limits of agreement (LoAs) were calculated as the mean ± 1.96 standard deviations (SD). Finally, the coefficient of determination (R^2) was calculated to observe the fit of the sample values to a regression line between the variables RE and ΔALP.

3. Results

The study includes 43 eyes, with a mean age of the participants of 72 ± 5.40 years [range: 68–84]. Table 1 displays both preoperative and postoperative parameters for each variable. There are no statistically significant differences (*t*-test, *p*-value > 0.05) between preoperative and postoperative parameters.

Table 1. Preoperative and postoperative data. Means ± SD [minimum value–maximum value].

	Preoperative Data	Postoperative Data	*p*-Value
AL (mm)	23.52 ± 0.96 [22.18–25.97]	23.46 ± 1.05 [22.06–25.97]	0.123
CCT (μm)	550 ± 37 [478–661]	550 ± 37 [475–654]	0.972
WTW (mm)	11.93 ± 0.36 [11.14–12.60]	11.95 ± 0.96 [10.9–12.89]	0.701
$K_{m\ anterior}$ (D)	43.23 ± 1.38 [40.65–46.44]	43.14 ± 1.44 [40.31–46.44]	0.572
$K_{m\ posterior}$ (D)	−5.97 ± 1.29 [(−6.5)–(−5.97)]	−6.16 ± 1.50 [(−6.60)–(−5.55)]	0.692
ACD (mm)	3.11 ± 0.38 [2.48–3.85]		
LT (mm)	4.52 ± 0.44 [3.470–5.450]	-	
ALP (mm)	-	4.53 ± 0.25 [3.81–5.24]	
IOLT (mm)	-	0.67 ± 0.06 [0.55–0.96]	
RE_{OBJ} (D)	−0.05 ± 0.35 [(−1.25)–(+1.00)]		
RE_{SUBJ} (D)	−0.02 ± 0.39 [(−0.62)–(+1.00)]		

AL, Axial Length; CCT, Central Corneal Thickness; WTW, White To White distance; $K_{m\ anterior}$, Mean Anterior keratometry; $K_{m\ posterior}$, Mean posterior keratometry; ACD, Anterior Chamber Depth; ALP, Actual Lens Position; LT, Crystalline Lens Thickness; IOLT, Intraocular Lens Thickness; RE_{OBJ}, Objective Refractive Error; RE_{SUBJ}, Subjective Refractive Error.

3.1. Intraocular Lens Power

Table 2 displays the differences between calculated and implanted IOLP. The average IOLP ± SD calculated with Hoffer Q, Holladay I, SRK/T, and Haigis are also shown. No significant differences were found between Hoffer Q, Holladay I, SRK/T, and Haigis (*t*-test, $p > 0.05$). Nevertheless, there were significant differences between the IOLP calculated and the implanted IOLP (calculated with Barrett Universal II) in all cases.

Table 2. Mean dif. between implanted and calculated IOLP using the formulas. The average IOLP calculated with Hoffer Q, Holladay I, SRK/T, and Haigis are shown in brackets.

		IOLP Hoffer Q [21.29 ± 2.79 D]	IOLP Holladay I [21.12 ± 2.72 D]	IOLP SRK/T [21.32 ± 2.50 D]	IOLP Haigis [21.12 ± 2.66 D]
Mean dif. ± SD (mm)	IOLP Implanted	0.31 ± 0.91	0.48 ± 1.01	0.28 ± 0.78	0.49 ± 0.83
LoAs (mm)		(−1.48, 2.10)	(−1.50, 2.47)	(−1.25, 1.81)	(−1.15, 2.12)
p-value (*t*-test)		0.030 *	0.003 *	0.023 *	$p < 0.001$ *

Mean dif., Mean of differences; SD, Standard Deviation; LoAs, Limits of agreement. * Statistically significant differences.

3.2. Effective Lens Position and Actual Lens Position

The predicted ELP for each formula was as follows: Hoffer Q = 5.53 ± 0.26 mm, Holladay I = 5.50 ± 0.31 mm, SRK/T = 5.78 ± 0.35 mm and Haigis = 4.92 ± 0.25 mm. The mean dif. between the ELP calculated with different formulas were illustrated in Table 3. The Haigis formula resulted in a smaller predicted ELP compared to the other formulas, and the difference was statistically significant (in all cases, $p < 0.05$). However, no statistically significant differences were found among the third-generation formulas. The mean ALP obtained using Lenstar in "pseudophakic" mode at 4–5 weeks after the surgery was 4.53 ± 0.25 mm in the range of [3.80–5.02] mm.

Table 3. Mean dif. between ELP calculated with Hoffer Q, Holladay I, SRK/T, and Haigis formulas.

		ELP Hoffer Q	ELP Holladay I	ELP SRK/T
Mean dif. ± SD (mm)	ELP Holladay I	0.02 ± 0.18	-	-
LoAs (mm)		(−0.32, 0.38)		
p-value (*t*-test)		0.320		

Table 3. *Cont.*

		ELP Hoffer Q	ELP Holladay I	ELP SRK/T
Mean dif. ± SD (mm)	ELP SRK/T	−0.04 ± 0.19	−0.07 ± 0.23	-
LoAs (mm)		(−0.42, 0.33)	(−0.52, 0.38)	
p-value (*t*-test)		0.139	0.055	
Mean dif. ± SD (mm)	ELP Haigis	0.61 ± 0.09	0.58 ± 0.22	0.65 ± 0.27
LoAs (mm)		(0.42, 0.79)	(0.14, 1.01)	(0.12, 1.17)
p-value (*t*-test)		0.001 *	$p < 0.001$ *	$p < 0.001$ *
Mean ± SD (mm)	ALP	4.53 ± 0.25		
range (mm)		(3.80–5.02)		

Mean dif., Mean of differences; SD, Standard Deviation; LoAs, Limits of agreement. * Statistically significant differences.

3.3. Optical Modeling

RE_{OSLO} was −0.03 ± 0.56 D in the range of [(−1.76)–(+1.21) D]. The results of the paired *t*-test between RE_{OSLO} and RE_{OBJ} was *p*-value = 0.660, and between RE_{OSLO} and RE_{SUBJ} were a *p*-value = 0.789, did not show any significant statistical differences between them.

Figure 2 shows Bland–Altman plots between RE_{OSLO} and RE_{OBJ} and between RE_{OSLO} and RE_{SUBJ}. Gray-filled regions were drawn to inform about ±0.25 D.

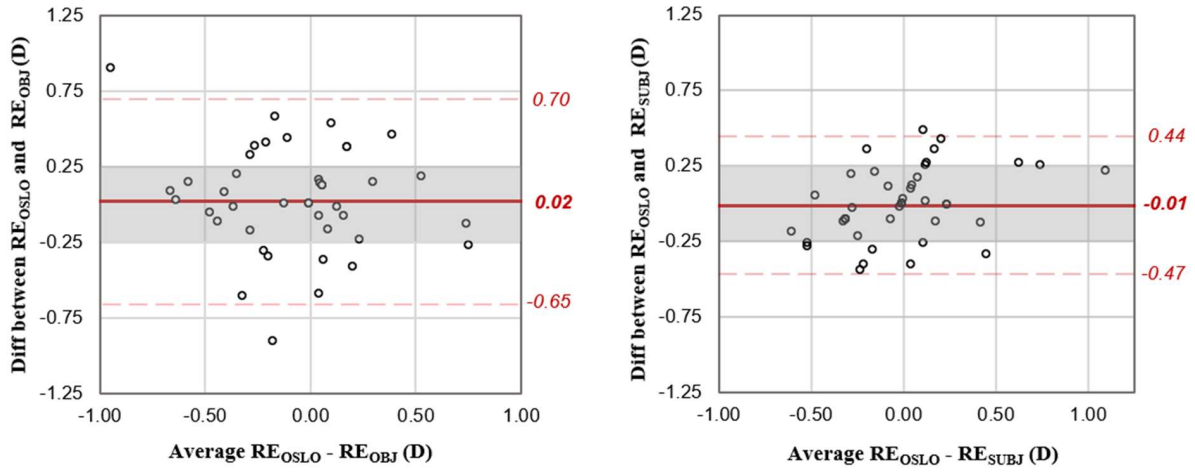

Figure 2. Bland–Altman plots between (**a**) RE_{OSLO} and RE_{OBJ} (**b**) RE_{OSLO} and RE_{SUBJ}. Mean dif. RE_{OSLO}-RE_{OBJ} = 0.02 ± 0.35 D and LoAs (−0.65, 0.70) D. Mean of dif. RE_{OSLO}-RE_{SUBJ} = −0.01 ± 0.27 D and LoAs (−0.47, 0.44) D. The gray area indicates ±0.25 D.

The ALP_{IDEAL} for achieving minimum RE_{OSLO} was 4.58 ± 0.48 mm in the range of [3.56–5.77] mm. There are statistically significant differences between ALP and ALP_{IDEAL} (*p*-value = 0.003). The ΔALP was −0.04 ± 0.45 mm with a range of [(−1)–1.20] mm. A positive value of ΔALP indicates that the IOL with that power should have been positioned closer to the cornea in order to achieve a RE_{OSLO} of 0 diopters. The study found a significant correlation between ΔALP and postoperative refractive errors (RE_{OBJ} and RE_{SUBJ}), describing a linear trendline equation of $y = 0.52x - 0.00$ ($R^2 = 0.46$) with RE_{OBJ} and $y = 0.59x + 0.02$ ($R^2 = 0.67$) with RE_{SUBJ}, as shown in Figure 3a,b. It is important to highlight the fact that eyes with large delta ALP (−1.00, +1.25 mm) will have large RE_{OBJ} and especially large RE_{SUBJ}, up to 1.00 diopter.

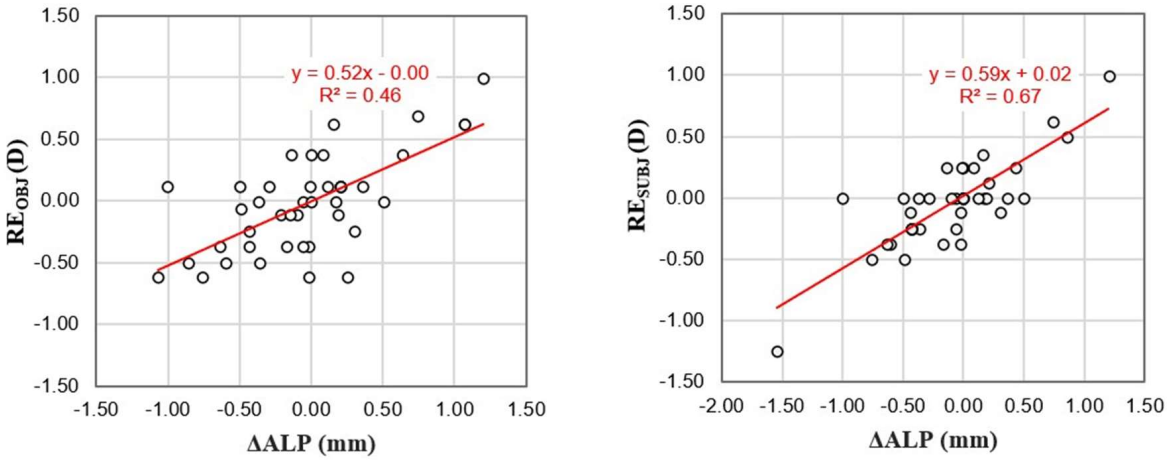

Figure 3. (**a**) RE_{OBJ} vs. ΔALP (mm). (**b**) RE_{SUBJ} vs. ΔALP (mm).

4. Discussion

Deviations in the preoperative estimation of postoperative IOL position, i.e., the ELP, represent the largest contribution to error in modern IOLP calculation formulas [2,16,22]. The current study analyzed the estimated ELP using various IOL power calculation formulas. Differences in the ELP calculated with Hoffer Q, Holladay I, and SRK/T were not statistically significant. However, the predicted ELP was consistently lower with the Haigis formula, which incorporates anterior chamber depth (ACD) in its estimation of ELP, compared to the other formulas. It has been observed that the accuracy of ELP calculations may vary among different calculation formulas and among individual patients.

Various authors have investigated parameters and formulas to accurately estimate the ELP and its correlation with the ALP [23,24]. Previous reports have shown discrepancies in theoretically back-calculating ELP compared to postoperative ALP [5,25,26]. Olsen and Hoffmann [27] proposed a C constant to estimate IOL position as a fraction of lens thickness. Hirnschall et al. [28] developed a regression equation using intraoperative measurements to predict postoperative IOL position. Over time, theoretical formulas for ELP calculation have evolved to incorporate additional biometric factors. However, factors such as IOL material, thickness, and optic-haptic configuration [29] also influence the final IOL position. Most theoretical IOL power calculation formulas are based on simplified eye models with thin corneas and IOL models [2].

In a previous study employing comparable methodology, Castro et al. [17] utilized Lenstar to measure postoperative ALP in patients who received the SN60WF IOL. Their findings closely mirrored ours, demonstrating an ALP of 4.50 ± 0.33 mm with the Clareon IOL, which shares the same platform design (Alcon Laboratories, Inc.). Moreover, Castro et al. [17] identified a 1.04 mm difference between ELP and ALP when using the SRK/T formula, a result that aligns with the 1.25 mm difference observed in our current study.

No statistically significant differences were identified between the IOLPs calculated using third-generation formulas and Haigis. However, there was a significant difference with Barrett Universal II, which incorporates additional parameters like LT, ACD, and WTW. Our study further confirms that using the Barrett formula is effective in calculating IOLP, as the mean of RE_{SUBJ} was −0.02 ± 0.39 D.

It is believed that among the factors affecting postoperative visual function, the stability of the postoperative IOL position has recently been considered a key factor. This stability can be represented by ELP [16]. Third-generation formulas ignore the posterior radius of the cornea and assume a single keratometric index. However, ray-tracing-based IOLP estimates can overcome these limitations. Customized ray-tracing eye models can integrate parameters such as anterior and posterior corneal topography, biometry and IOL position.

This approach can significantly improve the accuracy of IOLP selection, especially in challenging cases involving irregular corneas or eyes with prior refractive surgery.

In the present study, ray tracing was employed to model different eyes and adjust the theoretical positions of the IOLs to achieve emmetropia. To our knowledge, this is the first instance of using this tool for such a methodology and purpose. From Figure 2a,b, a strong correlation was found between RE_{OSLO} and RE_{SUBJ} [mean dif. -0.01 ± 0.27 D] and RE_{OSLO} and RE_{OBJ} [mean dif. 0.02 ± 0.35 D]. The SD for RE_{OSLO}-RE_{SUBJ} is closely aligned with the clinically significant tolerance of ± 0.25 D. It can be inferred that eye models developed using this tool, incorporating data from Lenstar and Pentacam, accurately depict the refractive characteristics of eyes post-cataract surgery.

This tool is proposed to study the impact of non-ideal axial positioning of the IOL. A strong correlation was found between RE_{SUBJ} and ΔALP, enabling the evaluation of different IOL positions to determine the most suitable position for calculations and optimize the study lens while assessing errors in magnitude and direction. In this context, an alternative approach could involve optimizing the IOLP for a specified position. However, a clinical constraint arises due to the standard availability of IOLs in 0.50 D increments.

This study has limitations. Firstly, the sample excluded eyes with extreme axial length. Secondly, only four open-source formulas were studied due to the unavailability of modern formulas like Barrett Universal II, which has an undisclosed ELP estimation method. Thirdly, the Clareon lens changes its design across a range from 16.50 to 26.50 D by varying the Coddington factor and clear optical zone, factors that were not taken into account. Additionally, refractive predictions using ray tracing relied on postoperative ALP measurements. Future studies should validate the tool preoperatively using formula-provided ELP estimates to anticipate potential errors and optimize IOL power calculation. Improving ELP prediction accuracy is crucial for achieving better refractive outcomes.

5. Conclusions

A customized ray-tracing eye model was proposed, integrating parameters such as anterior and posterior corneal topography, biometry, and IOL position. There is a strong correlation observed between different refractive parameters (RE_{OSLO}-RE_{SUBJ} and RE_{OSLO}-RE_{OBJ}), indicating the tool's ability to accurately predict refractive outcomes post-cataract surgery. Optical simulations were used to optimize ALP for emmetropia (ALP_{IDEAL}). There are statistically significant differences between ALP and ALP_{IDEAL}. A significant correlation between ΔALP ($\Delta ALP = ALP - ALP_{IDEAL}$) and RE_{SUBJ} was found, as well as between ΔALP and RE_{OBJ}.

Author Contributions: D.G.Y.—Data curation, formal analysis, investigation, methodology, project administration, supervision, validation, writing—original draft, writing—review and editing. L.R.M.—Formal analysis, funding acquisition, methodology, project administration, supervision, writing—original draft, writing—review and editing. F.J.C.A.—Conceptualization, investigation, methodology, supervision, project administration, writing—review and editing. I.P.E.—Conceptualization, data curation, formal analysis, investigation, methodology. All authors have read and agreed to the published version of the manuscript.

Funding: This research received no external funding.

Institutional Review Board Statement: The study was conducted in accordance with the Declaration of Helsinki and approved by Aragon Research Ethics Committee (CEICA).

Informed Consent Statement: Informed consent was obtained from all subjects involved in the study.

Data Availability Statement: The datasets generated and/or analyzed during the current study are not publicly available in order to avoid compromising individual privacy but are available from the corresponding author on reasonable request.

Acknowledgments: Diana Gargallo was supported by Gobierno de Aragón.

Conflicts of Interest: The authors declare no conflicts of interest.

References

1. Davis, G. The Evolution of Cataract Surgery. *Mo. Med.* **2016**, *113*, 58–62.
2. Olsen, T. Calculation of intraocular lens power: A review. *Acta Ophthalmol. Scand.* **2007**, *85*, 472–485. [CrossRef]
3. Norrby, S. Sources of error in intraocular lens power calculation. *J. Cataract. Refract. Surg.* **2008**, *34*, 368–376. [CrossRef] [PubMed]
4. Retzlaff, J.A.; Sanders, D.R.; Kraff, M.C. Development of the SRK/T intraocular lens implant power calculation formula. *J. Cataract. Refract. Surg.* **1990**, *16*, 333–340. [CrossRef] [PubMed]
5. Holladay, J.T.; Musgrove, K.H.; Prager, T.C.; Lewis, J.W.; Chandler, T.Y.; Ruiz, R.S. A three-part system for refining intraocular lens power calculations. *J. Cataract. Refract. Surg.* **1988**, *14*, 17–24. [CrossRef] [PubMed]
6. Hoffer, K.J. The Hoffer Q formula: A comparison of theoretic and regression formulas. *J. Cataract. Refract. Surg.* **1993**, *19*, 700–712. [CrossRef] [PubMed]
7. Barrett, G.D. An improved universal theoretical formula for intraocular lens power prediction. *J. Cataract. Refract. Surg.* **1993**, *19*, 713–720. [CrossRef]
8. Haigis, W. The Haigis formula. In *Intraocular Lens Power Calculations*; Shammas, H., Ed.; SLACK Incorporated: San Francisco, CA, USA, 2004; pp. 41–57.
9. Olsen, T.; Olesen, H.; Thim, K.; Corydon, L. Prediction of postoperative intraocular lens chamber depth. *J. Cataract. Refract. Surg.* **1990**, *16*, 587–590. [CrossRef] [PubMed]
10. Einighammer, J.; Oltrup, T.; Bende, T.; Jean, B. Calculating intraocular lens geometry by real ray tracing. *J. Refract. Surg.* **2007**, *23*, 393–404. [CrossRef]
11. Li, T.; Stein, J.; Nallasamy, N. AI-powered effective lens position prediction improves the accuracy of existing lens formulas. *Br. J. Ophthalmol.* **2022**, *106*, 1222–1226. [CrossRef]
12. Li, T.; Reddy, A.; Stein, J.D.; Nallasamy, N. Ray tracing intraocular lens calculation performance improved by AI-powered postoperative lens position prediction. *Br. J. Ophthalmol.* **2023**, *107*, 483–487. [CrossRef] [PubMed]
13. Kothari, S.S.; Reddy, J.C. Recent developments in the intraocular lens formulae: An update. *Semin. Ophthalmol.* **2022**, *38*, 143–150. [CrossRef] [PubMed]
14. Melles, R.B.; Kane, J.X.; Olsen, T.; Chang, W.J. Update on intraocular lens calculation formulas. *Ophthalmology* **2019**, *126*, 1334–1335. [CrossRef]
15. Holzer, M.P.; Mamusa, M.; Auffarth, G.U. Accuracy of a new partial coherence interferometry analyser for biometric measurements. *Br. J. Ophthalmol.* **2009**, *93*, 807–810. [CrossRef]
16. Cruysberg, L.P.J.; Doors, M.; Verbakel, F.; Berendschot, T.T.J.M.; De Brabander, J.; Nuijts, R.M.M.A. Evaluation of the Lenstar LS 900 non-contact biometer. *Br. J. Ophthalmol.* **2010**, *94*, 106–110. [CrossRef] [PubMed]
17. Castro-Alonso, F.J.; Bordonaba-Bosque, D.; Piñero, D.P.; Latre-Rebled, B. Predictive value of intracrystalline interphase point measured by optical low-coherence reflectometry for the estimation of the anatomical position of an intraocular lens after cataract surgery. *J. Cataract. Refract. Surg.* **2019**, *45*, 1294–1304. [CrossRef] [PubMed]
18. Atchison, D.A. Optical models for human myopic eyes. *Vis. Res.* **2006**, *46*, 2236–2250. [CrossRef] [PubMed]
19. Thibos, L.N.; Hong, X.; Bradley, A.; Cheng, X. Statistical variation of aberration structure and image quality in a normal population of healthy eyes. *J. Opt. Soc. Am. A* **2002**, *19*, 2329–2348. [CrossRef]
20. Thibos, L.N.; Horner, D. Power vector analysis of the optical outcome of refractive surgery. *J. Cataract. Refract. Surg.* **2001**, *27*, 80–85. [CrossRef] [PubMed]
21. Iskander, D.R.; Davis, B.A.; Collins, M.J.; Franklin, R. Objective refraction from monochromatic wavefront aberrations via Zernike power polynomials. *Ophthalmic Physiol. Opt.* **2007**, *27*, 245–255. [CrossRef]
22. Shammas, J.H.; Shammas, M.C. Improving the preoperative prediction of the anterior pseudophakic distance for intraocular lens power calculation. *J. Cataract. Refract. Surg.* **2015**, *41*, 2379–2386. [CrossRef] [PubMed]
23. Goto, S.; Maeda, N.; Koh, S.; Ohnuma, K.; Hayashi, K.; Iehisa, I.; Noda, T.; Nishida, K. Prediction of postoperative intraocular lens position with angle-to-angle depth using anterior segment optical coherence tomography. *Ophthalmology* **2016**, *123*, 2474–2480. [CrossRef] [PubMed]
24. Fernández, J.; Rodríguez-Vallejo, M.; Martínez, J.; Tauste, A.; Piñero, D.P. New approach for the calculation of the intraocular lens power based on the fictitious corneal refractive index estimation. *J. Ophthalmol.* **2019**, *2019*, 2796126. [CrossRef] [PubMed]
25. Gatinel, D.; Debellemanière, G.; Saad, A.; Dubois, M.; Rampat, R. Determining the theoretical effective lens position of thick intraocular lenses for machine learning–based iol power calculation and simulation. *Transl. Vis. Sci. Technol.* **2021**, *10*, 27. [CrossRef] [PubMed]
26. Holladay, J.T.; Maverick, K.J. Relationship of the actual thick intraocular lens optic to the thin lens equivalent. *Arch. Ophthalmol.* **1998**, *126*, 339–347. [CrossRef] [PubMed]
27. Olsen, T.; Hoffmann, P. C constant: New concept for ray tracing–assisted intraocular lens power calculation. *J. Cataract. Refract. Surg.* **2014**, *40*, 764–773. [CrossRef] [PubMed]

28. Hirnschall, N.; Amir-Asgari, S.; Maedel, S.; Findl, O. Predicting the postoperative intraocular lens position using continuous intraoperative optical coherence tomography measurements. *Investig. Ophthalmol. Vis. Sci.* **2013**, *54*, 5196–5203. [CrossRef]
29. Pereira, S.; Ganesh, S.; Umarani, R.; Sute, S.S. Prediction of effective lens position (ELP) and its changes in different monofocal intraocular lens (IOL's). *Glob. J. Cataract. Surg. Res. Ophthalmol.* **2023**, *1*, 93–98. [CrossRef]